DOI: 10.1007/s12541-013-0215-7

Thermo-mechanical Coupled Analysis of Automotive Brake Disc

Ali-Belhocine[1,#] and Mostefa-Bouchetara[1]

1 Department of Mechanical Engineering, USTOMB University, LP1505, El Mnaouer, USTO, Oran, Algeria, 31000(Zip code)
Corresponding Author / E-mail: al.belhocine@yahoo.fr, TEL: +213-793-851-317

KEYWORDS: Brake discs, Heat flux, Heat transfer coefficient, Von Mises stress, Contact pressure

This study aims to analysis the thermo-mechanical behavior at dry contact between disc and pad during braking phase by computer simulation. The geometric design model of disc analyzed at transient temperature to embody the ventilation system in vehicle. Deformation, Von Mises stress and contact pressures at pad are investigated by coupled thermo-mechanical. These simulation results are satisfactorily verified by comparing with similar literature result. Thus, this study provides effective reference for design and engineering application of brake disc and brake pad.

Manuscript received: December 18, 2012 / Accepted: June 04, 2013

NOMENCLATURE

a = Deceleration of the vehicle [ms^{-2}]
A_d = Disc surface swept by a brake pad [m^2]
g = Acceleration of gravity (9.81) [ms^{-2}]
m = Mass of the vehicle [kg]
q_0 = Entering heat flux [W]
v_0 = Initial speed of the vehicle [ms^{-1}]
$z = a/g$ = Braking effectiveness
ε_p = Factor load distribution on the disc surface
ϕ = Rate distribution of the braking forces between the front and rear axle

1. Introduction

Passenger cars have been one of the essential transportation for people to travel from one destination to another. The braking system represents one of the most fundamental safety-critical components in modern passenger cars. Therefore, the braking system of a vehicle is undeniably important, especially in slowing or stopping the rotation of a wheel by pressing brake pads against rotating wheel discs. Braking performance of a vehicle can significantly be affected by the temperature rise in the brake components. The frictional heat generated on the interface of the disc and the pads can cause high temperature. Particularly, the temperature may exceed the critical value for a given material, which leads to undesirable effects, such as brake fade, local scoring, thermo elastic instability, premature wear, brake fluid vaporization, bearing failure, thermal cracks, and thermally excited vibration.[1] Light weight advanced composite materials for vehicle application has been identified in order to reduce fuel consumption in the automobile systems. Over 75% of fuel consumption relates directly to vehicle weight. However, reducing the vehicle weight can improve the cost to performance ratio for the transportation industry. Researchers have shown that the vehicle weight reduction is a promising strategy for improving energy consumption in vehicles, and presents an important opportunity to reduce energy use in the transportation sector.[2]

The friction heat generated between two sliding bodies causes thermoelastic deformation which alters the contact pressure distribution. This coupled thermo-mechanical process is referred to as frictionally-excited thermoelastic instability or TEI.[3] If the sliding speed is above one called critical speed, the resulting thermo-mechanical feedback is unstable, leading to the development of non-uniform contact pressure and local high temperature with important gradients called 'hot spots'.[4] The formation of such localized hot spots is accompanied by high local stresses that can lead to material degradation and eventual failure.[5] Also, the hot spots can be a source of undesirable frictional vibrations, known in the automotive disc brake community as 'hot roughness' or 'hot judder'.[6]

In 2002, Nakatsuji et al.[7] conducted a study on the initiation of hair-like cracks which are formed around small holes in the flanges of one-

piece discs during overloading conditions. The study showed that thermally induced cyclic stress strongly affects the crack initiation in the brake discs. In order to show the crack initiation mechanism, the temperature distribution at the flange was firstly measured. The temperature distribution under overloading was analyzed by using the finite element method. Based on the experimental and calculated results, the crack initiation mechanism for one-piece brake discs at the very severe braking condition was explained. In addition, the effective methods are suggested for reducing the initiation of tiny cracks around the holes.

In 2000, Valvano and Lee[8] conducted a study of the technique to determine the thermal distortion of a brake rotor. The severe thermal distortion of a brake rotor can affect important brake system characteristics such as the system response and brake judder propensity. As such, the accurate prediction of thermal distortions can help in the designing of a brake disc.

In 1997, Hudson and Ruhl[9] conducted a study of the air flow through the passage of a Chrysler LH platform-ventilated brake rotor. Modifications to the production rotor's vent inlet geometry were prototyped and measured, in addition to the production rotor. Vent passage air flow was compared with the existing correlations. With the aid of Chrysler Corporation, investigation of ventilated brake rotor vane air flow was undertaken. The goal was to measure current vane air flow and to improve this vane flow to increase brake disc cooling.

Temperature increases can strongly influence the properties of the surface of materials in slip, support physicochemical and microstructural transformations, and modify the rheology of interfacial elements trapped in the contact zone.[10] Recent numerical models, presented to deal with rolling processes[11,12] have shown that the thermal gradients can attain important levels which depend on the heat dissipated by friction, the rolling speed, and the heat transfer coefficient. Many other studies[13,14] dealt with the evaluation of temperature in solids subjected to frictional heating. The temperature distribution due to friction process necessitates a good knowledge of the contact parameters. In fact, the interface is always imperfect–due to the roughness – from mechanical and thermal points of view. Recently, theoretical and experimental studies[15,16] have been developed to characterize the thermal parameters which govern the heat transfer at the vicinity of a sliding interface. In certain industrial applications, the solids are provided with a surface coating. A recent study has been carried out to analyze the effect of surface coating on the thermal behavior of a solid subjected to the friction process.[17] Increased thermal efficiency and the integrity of materials in high-temperature environments is an essential requirement in modem engineering structures in automotive, aerospace, nuclear, offshore, environmental, and other industries. Nowadays, the FE method is used regularly to obtain numerical solutions for heat transfer problems. The most common choice when using finite elements is the standard Galerkin formulation.[18]

Gao and Lin[19] stated that there is considerable evidence that shows the contact temperature is an integral factor reflecting the specific power friction influence of combined effect of load, speed, friction coefficient, and the thermo physical and durability properties of the materials of a frictional couple.

Talati and Jalalifar[20] presented a paper on Analysis of heat conduction in a disc brake system. In this paper, the governing heat equations for the disc and the pad are extracted in the form of transient heat equations with heat generation that is dependant to time and space. In the derivation of the heat equations, parameters such as the duration of braking, vehicle velocity, geometries and the dimensions of the brake components, materials of the disc brake rotor and the pad and contact pressure distribution have been taken into account. The problem is solved analytically using Green's function approach. It is concluded that the heat generated due to friction between the disc and the pad should be ideally dissipated to the environment to avoid decreasing the friction coefficient between the disc and the pad and to avoid the temperature rise of various brake components and break fluid vaporization due to excessive heating.

Naji et al.[21] presented a mathematical model to describe the thermal behavior of a brake system which consists of the shoe and the drum. The model is solved analytically using Green's function method for any type of the stopping braking action. The thermal behavior is investigated for three specified braking actions which were the impulse, the unit step and trigonometric stopping actions.

Thermal response of disc brake systems to different materials used for the disc-pad couple has been studied in many researches.[22-29] Aerodynamic cooling of high performance disc brake systems is investigated by many researchers.[30-32]

Kang and Cho[33] were conducted to analyze the geometry of vents in motorcycle disc brakes which affects the surface of the disc. To analyze the thermal characteristics of disc brakes, thermal deformation analysis and thermal stress analysis due to heat transfer was carried out through the finite element analysis for ventilated disc and full disc. For 3-dimensional modeling and finite element analysis of the discs, the commercial code ANSYS Workbench was used.

Thilak VMM et al.[34] conducted a transient thermal and structural analysis of a brake disc to evaluate its performance under severe braking conditions and there by assist in disc rotor design and analysis. The usage of new materials was investigated which aims at improving the braking efficiency and providing greater stability to the vehicle. This study was done using ANSYS 11 software to analyze the temperature distribution, variation of the stresses and deformation across the disc brake profile. The new materials under study were Aluminum base metal matrix composite and High Strength Glass Fiber composites. These materials have a promising friction and wear behavior as a brake disc. The transient thermo elastic analysis of discs in repeated brake applications was performed and the results were compared to that of cast iron disc.

Lee and Yeo[35] reported that uneven distribution of temperature at the surfaces of the disc and friction pads brings about thermal distortion, which is known as coning and found to be the main cause of judder and disc thickness variation (DTV). Ouyang et al[36] in their recent work found that temperature could also affect vibration level in a disc brake assembly.

In a recent work, Ouyang et al[36] and Hassan et al[37] employed finite element approach to investigate thermal effects on disc brake squeal using dynamic transient and complex eigenvalue analysis, respectively. Braking system is the single most important safety feature of every vehicle on the road. The ability of the braking system to bring a vehicle to safe controlled stop is absolutely essential in preventing accidental vehicle damage and personal injury. The braking system is composed

of many parts, including friction pads on each wheel, a master cylinder, wheel cylinders, and a hydraulic control system.[38]

Disc brake consists of cast-iron disc which rotates with the wheel, caliper fixed to the steering knuckle and friction material (brake pads). When the braking process occurs, the hydraulic pressure forces the piston and therefore pads and disc brake are in sliding contact. Set up force resists the movement and the vehicle slows down or eventually stops. Friction between disc and pads always opposes motion and the heat is generated due to conversion of the kinetic energy.[39] The three-dimensional simulation of thermo-mechanical interactions on the automotive brake, showing the transient thermo-elastic instability phenomenon, is presented for the first time in this academic community.[40]

In the study established in 2012 by Park et al.,[41] an analysis technique that can estimate the temperature rise and thermal deformation of the ventilated disc considering vehicle information, braking condition and properties of the disc and pad was developed. The analytical process of the braking power generation during braking was mathematically derived. The thermal energy that is applied to the surface of a disc as heat flux was calculated when a vehicle is decelerating from 130 km/h to 0 km/h with deceleration of 0.4 g. Then, the temperature rise and thermal deformation of a disc are calculated through the thermo-mechanical analysis by using SAMCEF code. The shape of the cross section of the disc is optimized according to the response surface analysis method in order to minimize the temperature rise and thermal deformation.

Design parameters of the ventilated disc are optimized according to the response surface analysis method.[42-45] The optimization result is validated by performing the hot judder analysis11 of the original and optimized disc brake models.

In the study carried out by Chung et al.,[46] a transient FE analysis method was used to analyze the full coupled thermoelastic instability problem for a disc brake system. The three dimensional mechanical and thermal models for the disc brake were generated separately, and solved iteratively using the staggered approach The simulation results such as the maximum disc temperature, BTV are compared to the data from the dynamo test, and the reliabilities of the analysis technique and simulation model are verified.

In this study, we will make a modeling of the thermo-mechanical behavior of the dry contact between the discs of brake pads at the time of braking phase; the strategy of calculation is based on the software ANSYS 11.[47] This last is comprehensive mainly for the resolution of the complex physical problems. The numerical simulation of the coupled transient thermal field and stress field is carried out by sequentially thermal-structurally coupled method based on ANSYS.

2. Heat flux entering the disc

The brake disc consumes the major part of the heat, usually grater than 90%,[48] by means of the effective contact surface of the friction coupling. Considering the complexity of the problem and the limitation in the average data processing, one identifies the pads by their effect, represented by an entering heat flux (Fig. 1).

The initial heat flux q_0 entering the disc is calculated by the following formula:[49]

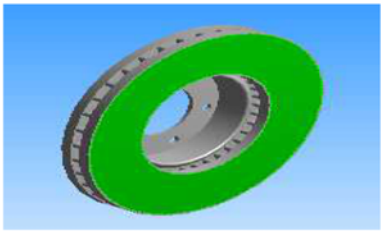

Fig. 1 Application of flux

Table 1 Parameters of automotive brake application

Inner disc diameter, mm	66
Outer disc diameter, mm	262
Disc thickness (TH), mm	29
Disc height (H), mm	51
Vehicle mass m, kg	1385
Initial speed v_0, km/h	28
Deceleration a, m/s^2	8
Effective rotor radius R_{rotor}, mm	100.5
Rate distribution of the braking forces Φ, %	20
Factor of charge distribution of the disc ε_p	0.5
Surface disc swept by the pad A_d, mm^2	35993

Table 2 Thermoelastic properties used in simulation

Material Properties	Pad	Disc
Thermal conductivity, k (w/m. ^{o}C)	5	57
Density, ρ (kg/m^3)	1400	7250
Specific heat, c (J/Kg. ^{o}C)	1000	460
Poisson's ratio, v	0.25	0.28
Thermal expansion, α (10^{-6} / ^{o}C)	10	10.85
Elastic modulus, E (GPa)	1	138
Coefficient of friction, μ	0.2	0.2
Operation Conditions		
Angular velocity, ω (rd/s)		157.89
Hydraulic pressure, P (MPa)		1

$$q_0 = \frac{1-\varnothing}{2}\frac{mgv_0 z}{2A_d\varepsilon_p} \quad (1)$$

The loading corresponds to the heat flux on the disc surface. The dimensions and the parameters used in the thermal calculation are recapitulated in Table 1.

The disc material is gray cast iron (GFC) with high carbon content,[50] with good thermophysical characteristics, and the brake pad has an isotropic elastic behavior, thermo-mechanical characteristics of which adopted in this simulation in one of the two parts are recapitulated in Table 2.

3. Modeling in ANSYS CFX

The finite volume method consists of three stages: the formal integration of the governing equations of the fluid flow over the entire (finite) control volumes of the solution domain. Then, discretization, involving the substitution of a variety of finite-difference-type approximations for the terms in the integrated equation representing flow processes such as convection, diffusion, and sources. This

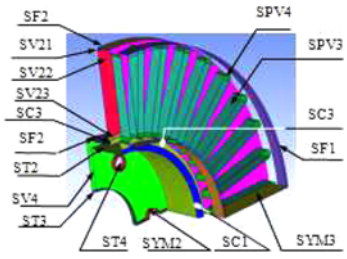

Fig. 2 Definition of surfaces of the ventilated disc

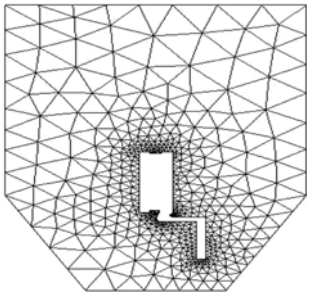

Fig. 3 Irregular mesh in the wall

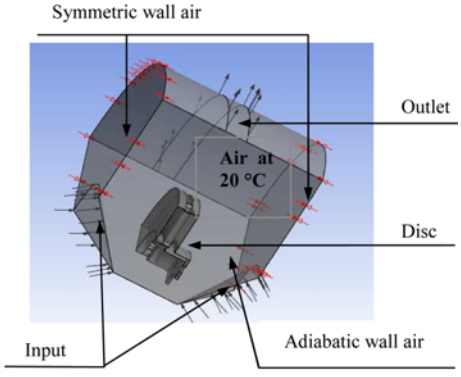

Fig. 4 Brake disc CFD model

converts the integral equation into a system of algebraic equations, which can then be solved using iterative methods.[51] The first stage of the process, the control volume integration, is the step that distinguishes the finite volume method from other CFD methods. The statements resulting from this step express the "exact" conservation of the relevant properties for each finite cell volume. This gives a clear relationship between the numerical analog and the principle governing the flow. To enable the modeling of a rotating body (in this case the disc), the code employs the rotating reference frame technique. For the preparation of the mesh of CFD model, one defines initially, various surfaces of the disc in ICEM CFD as shown in Fig. 2; we used a linear tetrahedral element with 30717 nodes and 179798 elements. In order not to weigh down calculation, an irregular mesh is used in which the mesh is broader where the gradients are weaker (nonuniform mesh), (Fig. 3).

The CFD models were constructed and were solved using ANSYS-CFX software package.[52] The model applies periodic boundary conditions on the section sides. As the brake disc is made from sand-casted grey cast iron, the disc model is attached to an adiabatic shaft, the axial length of which spans that of the domain. Air around the disc is considered to be 20°C, and open boundaries with zero relative pressure were used for the upper, lower, and radial ends of the domain.

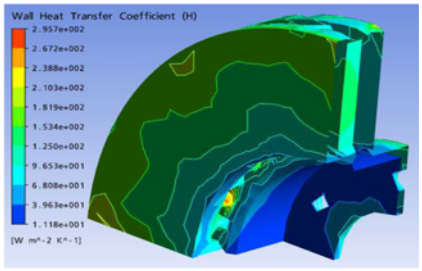

Fig. 5 Distribution of heat-transfer coefficient on a ventilated disc in the stationary case (FG 15)

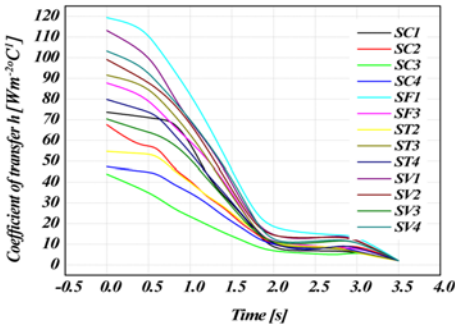

Fig. 6 Variation of heat-transfer coefficient *(h)* of various surfaces for a full disc in the nonstationary case (FG 15)

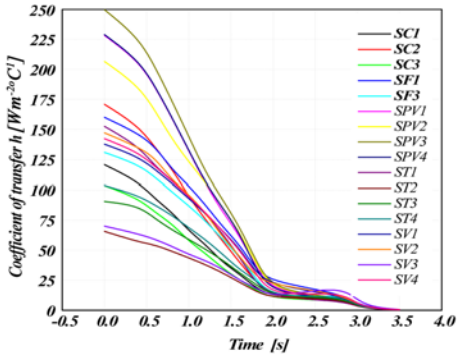

Fig. 7 Variation of heat-transfer coefficient *(h)* of various surfaces for a ventilated disc in transient case (FG 15)

Material data were taken from ANSYS material data library for air at 20°C. Reference pressure was set to be 1 atm, low turbulence intensity, and the turbulent model used was k-ε. (Fig. 4).

The airflow through and around the brake disc was analyzed using the ANSYS-CFX software package. The ANSYS-CFX solver automatically calculates heat-transfer coefficient at the wall boundary. Afterwards the heat-transfer coefficients considering convection were calculated and organized in such a way, that they could be used as a boundary condition in thermal analysis. Averaged heat-transfer coefficient had to be calculate for all disc using ANSYS-CFX Post as it is indicated in Fig. 5.

From the comparison between Figs. 6 and 7 concerning the variation of heat-transfer coefficients in the nonstationary mode for the two types of design, full and ventilated, one notes that the introduction of the system of ventilation directly influences the value of this coefficient for same surface, which is logically significant because this mode of ventilation results in the reduction in the differences of wall-fluid temperature.

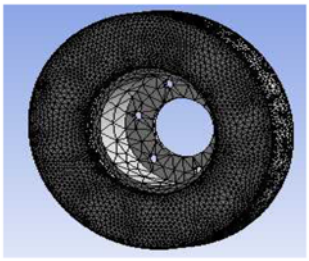

(a) Full disc (172103 nodes - 114421 elements)

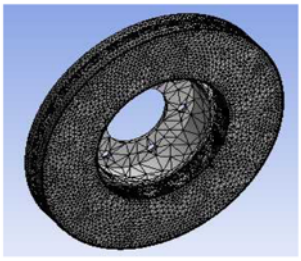

(b) Ventilated disc (154679 nodes - 94117 elements)

Fig. 8 Meshing of the disc

4. Meshing of the disc

The elements used for the mesh of the full and ventilated disc are tetrahedral 3D elements with 10 nodes (isoperimetric) (Fig. 8).

5. Initial and boundary conditions

The boundary conditions are introduced into module ANSYS Workbench [Multiphysics], by choosing the mode of first simulation of the all (permanent or transitory), and by defining the physical properties of materials. These conditions constitute the initial conditions of our simulation. After having fixed these parameters, one introduces a boundary condition associated with each surface

- Total time of simulation = 45 s
- Increment of initial time = 0.25 s
- Increment of minimal initial time = 0.125 s
- Increment of maximal initial time = 0.5 s
- Initial temperature of the disc = 60°C
- Materials: Grey Cast iron FG 15.
- Convection: One introduces the values of the heat-transfer coefficient *(h)* obtained for each surface in the shape of a curve (Figs. 6, 7)
- Flux: One introduces the values obtained by flux entering by means of the code CFX.¶

6. Results and discussions

6.1 Influence of construction of the disc

Figs. 9 and 10 show the variation in the temperature according to time during the simulation. From the first step, the variation in the temperature shows a great growth which is due to the speed of the physical course of the phenomenon during braking, namely friction, plastic microdistortion of contact surfaces.

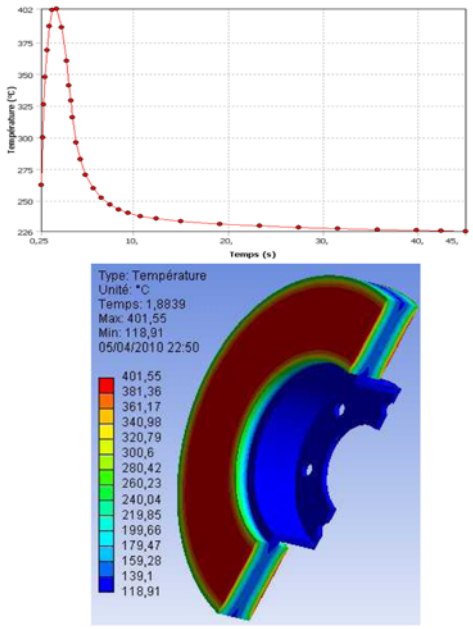

$t = 1.8839$ s, $T_{max} = 401.66$°C

Fig. 9 Temperature distribution of a full disc of cast iron (FG 15)

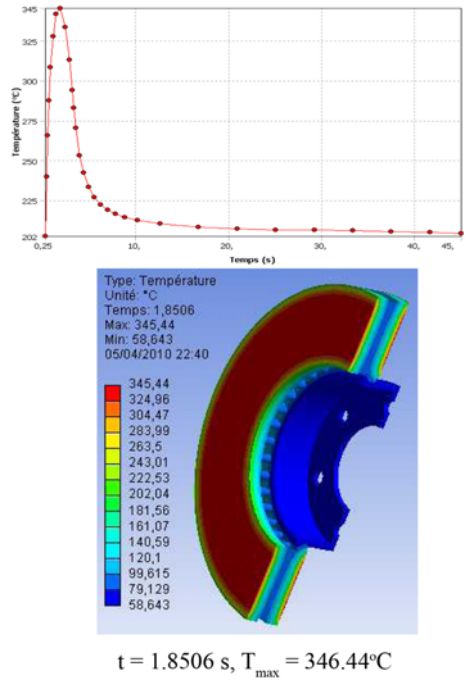

$t = 1.8506$ s, $T_{max} = 346.44$°C

Fig. 10 Temperature distribution of a ventilated disc of cast iron (FG 15)

For the full disc, the temperature reaches its maximum value of 401.55°C at the moment $t = 1.8839$ s, and then it falls rapidly up to 4.9293 s—as from this moment and up to the end ($t = 45$ s) of simulation, the variation in the temperature become slow. It is noted that the interval [0-3.5] s represents the phase of forced convection.

During this phase, one observes the case of the free convection until the end of the simulation. In the case of the ventilated disc, one observes that the temperature of the disc falls approximately by 60°C compared with the first case. It is noted that ventilation in the design of the discs of brake plays an important role in producing a better system of cooling.

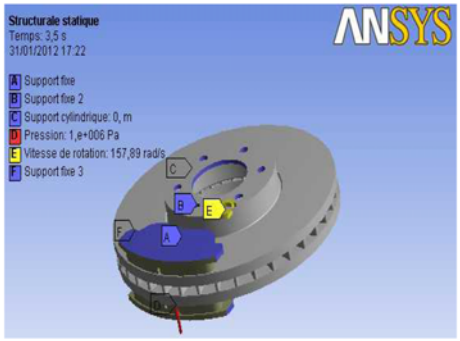

Fig. 11 Boundary conditions and loading imposed on the disc-pads

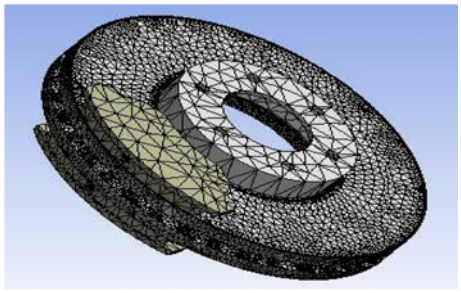

Fig. 12 Refined mesh of the model

7. Coupled Thermo-mechanical Analysis

7.1 FE model and boundary conditions

The purpose of the analysis is to predict the temperatures and corresponding thermal stresses in the brake disc when the vehicle is subjected to sudden high speed stops as can occur under autobahn driving conditions.[53] A commercial front disc brake system consists of a rotor that rotates about the axis of a wheel, a caliper–piston assembly where the piston slides inside the caliper, which is mounted to the vehicle suspension system, and a pair of brake pads. When hydraulic pressure is applied, the piston is pushed forward to press the inner pad against the disc, and simultaneously the outer pad is pressed by the caliper against the disc.[54] In a real car disc brake system, the brake pad surface is not smooth at all. Abu Bakar and Ouyang[55] adjusted the surface profiles using measured data of the surface height and produced a more realistic model for brake pads. Fig. 11 shows the FE model and boundary conditions embedded configurations of the model composed of a disc and two pads. The initial air temperature of the disc and pads is 20°C, and the surface convection condition is applied at all surfaces of the disc, and the convection coefficient *(h)* of 5 W/m^2°C is applied to the surfaces of the two pads. The FE mesh is generated using 3D tetrahedral element with 10 nodes (solid 187) for the disc and pads. Overall, 185901 nodes and 113367 elements are used (Fig. 12).

In this study, a transient thermal analysis will be carried out to investigate the temperature variation across the disc using ANSYS software. Further structural analysis will also be carried out by coupling thermal analysis.

7.2 Thermal deformation

Fig. 13 gives the distribution of the total distortion in the whole (disc-pads) for various moments of simulation. For this figure, the scale

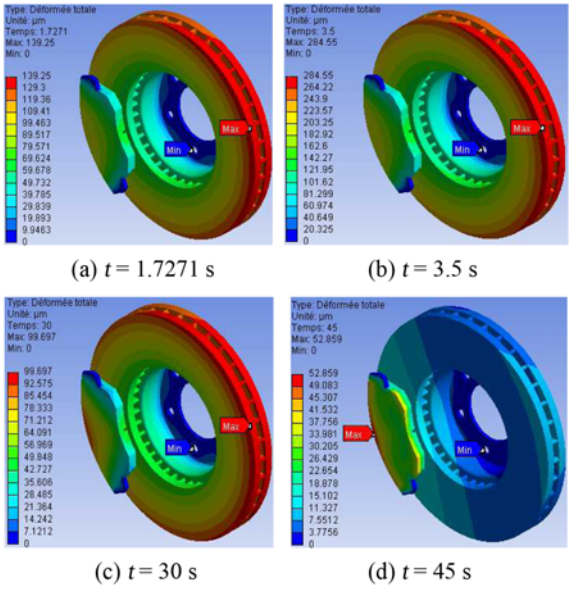

(a) $t = 1.7271$ s (b) $t = 3.5$ s

(c) $t = 30$ s (d) $t = 45$ s

Fig. 13 Total distortion distribution

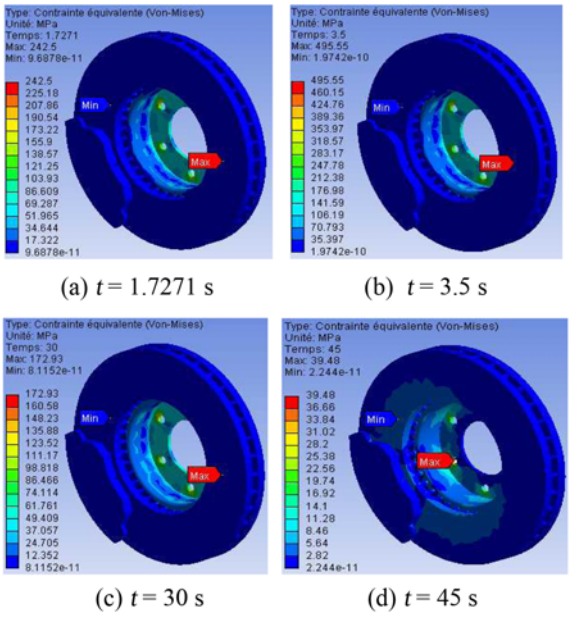

(a) $t = 1.7271$ s (b) $t = 3.5$ s

(c) $t = 30$ s (d) $t = 45$ s

Fig. 14 Von Mises stress distribution

of values of the deformation varies from 0 to 284.55 *µm. The* The value of the maximum displacement recorded during this simulation is at the moment, $t = 3.5$ s, which corresponds to the time of braking. One observes a strong distribution which increases with time on the friction tracks, and the crown external and the cooling fins of the disc. ¶Indeed, during a braking moment, the maximum temperature depends almost entirely on the heat storage capacity of disc (on particular tracks of friction); this deformation will generate an asymmetry of the disc following the rise of temperature which will cause a deformation in the shape of an umbrella.

7.3 Von Mises stress distribution

Fig. 14 presents the distribution of the constraint equivalent of Von Mises for various moments of simulation, the scale of values varying from 0 to 495.56 MPa. The maximum value recorded during this

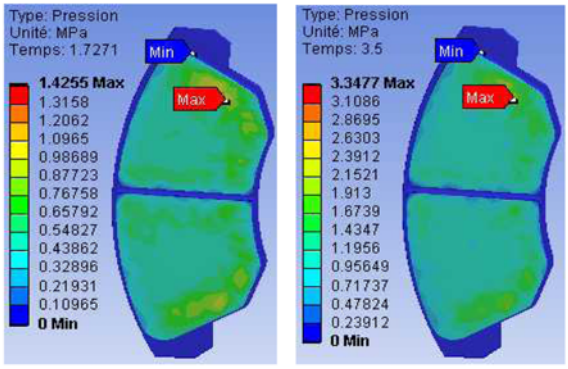

(a) $t = 1.7271$ s (b) $t = 3.5$ s

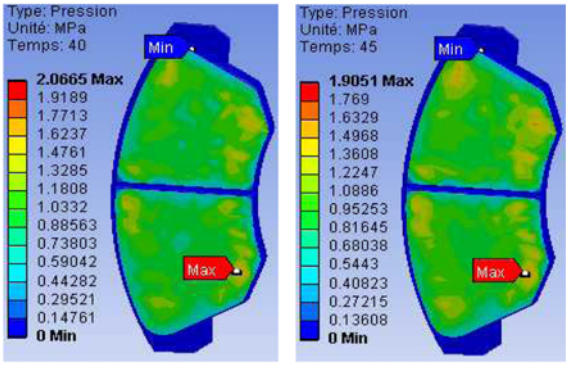

(c) $t = 40$ s (d) $t = 45$ s

Fig. 15 Contact pressure distribution in the inner pad

simulation of the thermo-mechanical coupling is very significant compared to that obtained with the assistance in the mechanical analysis dryness under the same conditions. One observes a strong constraint on the level of the bowl of the disc. Indeed, the disc is fixed to the hub of the wheel by screws, thus preventing its movement. Ini In the present of the rotation of the disc and the requests of torsional stress and sheers generated at the level of the bowl which are able to create the stress concentrations. The repetition of these effects lead to risks of rupture on the level of the bowl of the disc.

7.4 Contact pressure

Due to thermal deformation, contact area and pressure distribution also change. Thermal and mechanical deformations affect each other strongly and simultaneously.[56] As pressure distribution is another important aspect concerned in this research, it will be studied in the context of uneven temperature distributions. Contact analysis of the interfacial pressure in a disc brake without considering thermal effects was carried out in the past, for example, in Tirovic and Day.[57] Brake squeal analysis in recent years always includes a static contact analysis as the first part of the complex eigenvalue analysis.[58,59]

Fig. 15 shows the contact pressure distribution in the friction interface of the inner pad taken at various times of simulation. For this distribution, the scale varies from 0 to 3.3477 MPa and reached a value of pressure at the moment $t = 3.5$ s, which corresponds to the null rotational speed. It is also noticed that the maximum contact pressure is located on the edges of the pad decreasing from the leading edge toward the trailing edge from friction. This pressure distribution is almost symmetrical compared with the groove, and it has the same tendency as that of the distribution of the temperature because the highest area of the pressure is located in the same sectors. Indeed, at the time of the thermo-mechanical coupling of 3d, the pressure produces the symmetric field of the temperature. This last one affects thermal dilation and leads to a variation of the contact pressure distribution.

8. Conclusion

In this article, we have presented the analysis of the thermo-mechanical behavior of the dry contact between the brake disc, and pads during the braking process; the modeling is based on the ANSYS 11.0. We have shown that the ventilation system plays an important role in cooling the discs and provides a good high-temperature resistance. The analysis results showed that, temperature field and stress field in the process of braking phase were fully coupled. The temperature, Von Mises stress, and the total deformations of the disc and contact pressures of the pads increases as the thermal stresses are apart from the to mechanical stress which causes the crack propagation and fracture of the bowl and wear of the disc and pads. Regarding the calculation results, we can say that they are satisfactorily in agreement with those commonly found in the literature investigations. It would be interesting to solve the problem in thermo-mechanical disc brakes with an experimental study to validate the numerical results, for example, on test benches, in order to demonstrate a good agreement between the model and reality.

Regarding the outlook, there are three recommendations for the expansion of future work related to disc brake that can be done to further understand the effects of thermo-mechanical contact between the disc and pads, the recommendations are as follows:

1) Experimental study to verify the accuracy of the numerical model developed.
2) Tribological and vibratory study of the contact disc - pads;
3) Study of dry contact sliding under the macroscopic aspect (macroscopic state of the surfaces of the disc and pads).

REFERENCES

1. Bakar, A. R. A., Ouyang, H., Khai, L. C., and Abdullah, M. S., "Thermal Analysis of a Disc Brake Model Considering a Real Brake Pad Surface and Wear," International Journal of Vehicle Structures & Systems, Vol. 2, No. 1, pp. 20-27, 2010.

2. Maleque, M. A., Adebisi, A. A., and Shah, Q. H., "Energy and Cost Analysis of Weight Reduction using Composite Brake Rotor," International Journal of Vehicle Structures & Systems, Vol. 4, No. 2, pp. 69-73, 2012.

3. Lee, K. J. and Barber, J. R., "An Experimental Investigation of Frictionally-Excited Thermoelastic Instability in Automotive Disk Brakes Under a Drag Brake Application," J. Tribol, Vol. 116, pp. 409-414, 1994.

4. Altuzarra, O., Amezua, E., Aviles, R., and Hernandez, A., "Judder vibration in disc brakes excited by thermoelastic instability," Eng. comput, Vol. 19, No. 4, pp. 411-430, 2002.

5. Jang, Y. H. and Ahn, S. H., "Frictionally-excited thermoelastic instability in functionally graded material," Wear, Vol. 262, pp. 1102-1112, 2007.
6. Yi, B. Y., Barber, J. R., and Zagrodzki, P., "Eigenvalue solution of thermoelastic instability problems using Fourier reduction," Proc. R. Soc. London, A, Vol. 456, pp. 2799-282, 2000.
7. Nakatsuji, T., Okubo, K., Fujii, T., and Sasada, M., "Study on Crack Initiation at Small Holes of One-piece Brake Discs," SAE Technical Paper, Vol. 66, No. 646, pp. 2016-2023, 2002.
8. Valvano, T. and Lee, K., "An Analytical Method to Predict Thermal Distortion of a Brake Rotor," SAE Technical Paper, Vol. 109, No. 6, pp. 566-571, 2000.
9. Hudson, M. D. and Ruhl, R. L., "Ventilated Brake Rotor Air Flow Investigation," SAE Technical Paper, Vol. 106, No. 6, pp. 1862-1871, 1997.
10. Denape, J. and Laraqi, N., "Aspect thermique du frottement: mise en évidence expérimentale et éléments de modélisation," Mécanique & Industries, Vol. 1, No. 6, pp. 563-579., 2000.
11. Hamraoui, M., "Thermal behaviour of rollers during the rolling process," Applied Thermal Engineering, Vol. 29, No. 11-12, pp. 2386-2390, 2009.
12. Hamraoui, M. and Zouaoui, Z., "Modelling of heat transfer between two rollers in dry friction," Int. J. Therm. Sci., Vol. 48, No. 6, pp. 1243-1246, 2009.
13. Laraqi, N., "Velocity and relative contact size effect on the thermal constriction resistance in sliding solids," ASME J. Heat Transf., Vol. 119, pp. 173-177, 1997.
14. Yapýcý, H., Genç, M. S., and Özýsýk, G., "Transient temperature and thermal stress distributions in a hollow disk subjected to a moving uniform heat source," J. Therm. Stress., Vol. 31, pp. 476-493, 2008.
15. Laraqi, N., Alilat, N., de Maria, J. M., and Baïri, A., "Temperature and division of heat in a pin-on-disc frictional device – Exact analytical solution," Wear, Vol. 266, No. 7-8, pp. 765-770, 2009.
16. Bauzin, J. G. and Laraqi, N., "Simultaneous estimation of frictional heat flux and two thermal contact parameters for sliding contacts," Numerical Heat Transfer Part a-Applications, Vol. 45, No. 4, pp. 313-328, 2004.
17. Baïri, A., J. M. Garcia de Maria, n., and Laraqi, N., "Effect of thickness and physical properties of film on the thermal behavior of moving rough interfaces," The European Physical Journal - Applied Physics, Vol. 26, No. 1, pp. 29-34, 2004.
18. Mijuca, D. M., iberna A. M., and Medjo B. I., "A new multifield finite element method in steady state heat analysis," Therm. Sci. Vol. 9, No. 1, pp. 111-130, 2005.
19. Gao, C. H. and Lin, X. Z., "Transient temperature field analysis of a brake in a non-axisymmetric threedimensional model," J. Materials Processing Technology, Vol. 129, pp. 513-517, 2002.
20. Talati, F. and Jalalifar, S, "Analysis of heat conduction in a disk brake system," Heat and Mass Transfer, Vol. 45, No. 8, pp. 1047-1059, 2000.
21. Naji, M., Al-Nimr, M., and Masoud, S., "Transient thermal behavior of a cylindrical brake system," Heat and Mass Transfer, Vol. 36, No. 1, pp. 45-49, 2000.
22. Mosleh, M., Blau, P. J., and Dumitrescu, D., "Characteristics and morphology of wear particles from laboratory testing of disk brake materials," Wear, Vol. 256, No. 11-12, pp. 1128-1134, 2004.
23. Mutlu, I., Alma, M. H., Basturk, M. A., and Oner, C., "Preparation and characterization of brake linings from modified tannin-phenol formaldehyde resin and asbestos-free fillers," Journal of Materials Science, Vol. 40, No. 11, pp. 3003-3005, 2005.
24. Hecht, R. L., Dinwiddie, R. B., and Wang, H., "The effect of graphite flake morphology on the thermal diffusivity of gray cast irons used for automotive brake discs," Journal of Materials Science, Vol. 34, No. 19, pp. 4775-4781, 1999.
25. Gudmand-Høyer, L., Bach, A., Nielsen, G. T., and Morgen, P., "Tribological properties of automotive disc brakes with solid lubricants," Wear, Vol. 232, No. 2, pp. 168-175, 1999.
26. Uyyuru, R. K., Surappa, M. K., and Brusethaug, S., "Tribological behavior of Al-Si-SiCp composites/automobile brake pad system under dry sliding conditions," Tribology International, Vol. 40, No. 2, pp. 365-373, 2007.
27. Cho, M. H., Cho, K. H., Kim, S. J., Kim, D. H., and Jang, H., 'The Role of Transfer Layers on Friction Characteristics in the Sliding Interface between Friction Materials against Gray Iron Brake Disks," Tribology Letters, Vol. 20, No. 2, pp. 101-108, 2005.
28. Boz, M. and Kurt, A., "The effect of Al2O3 on the friction performance of automotive brake friction materials," Tribology International, Vol. 40, No. 7, pp. 1161-1169, 2007.
29. Blau, P. J. and McLaughlin, J. C., "Effects of water films and sliding speed on the frictional behavior of truck disc brake material," Tribology International, Vol. 36, No. 10, pp. 709-715, 2003.
30. McPhee, A. D. and Johnson, D. A., "Experimental heat transfer and flow analysis of a vented brake rotor," International Journal Thermal Sciences, Vol. 47, No. 4, pp. 458-467, 2008.
31. Wallis, L., Leonardi, E., Milton, B., and Joseph, P., "Air flow and heat transfer in ventilated disk brake rotors with diamond and tear-drop pillars," Numerical Heat Transfer Part A: Applications, Vol. 41, No. 6-7, pp. 643-655, 2002.
32. Johnson, D. A., Sperandei, B. A., and Gilbert, R., "Analysis of the Flow Through a Vented Automotive Brake Rotor," Journal of Fluids Engineering, Vol. 125, No. 6, pp. 979-986, 2004.
33. Kang, S. S. and Cho, S. K., "Thermal deformation and stress analysis of disk brakes by finite element method Journal of Mechanical Science and Technology," Vol. 26, No. 7, pp. 2133-2137, 2012.

34. Thilak, V. M. M., Krishnaraj, R., Sakthivel, M., and Kanthavel, K., Deepan marudachalam, M. G., Palani, R., "Transient thermal and structural analysis of the rotor disc of disc brake," International Journal of Scientific & Engineering Research, Vol. 2, No. 8, 2011.

35. Lee, S. and Yeo, T., "Temperature and coning analysis of brake rotor using an axisymmetric finite element technique," Proc. 4th Korea-Russia Int. Symp. On Science & Technology, Vol. 3, pp. 17-22, 2000.

36. Ouyang, H., Abu-Bakar, A. R., and Li, L., "A combined analysis of heat conduction, contact pressure and transient vibration of a disc brake," International Journal of Vehicle Design, Vol. 51, No. 1, pp. 190-206, 2009.

37. Hassan, M. Z., Brooks, P. C., and Barton, D. C., "A predictive tool to evaluate disk brake squeal using a fully coupled thermo-mechanical finite element model," International Journal of Vehicle Design, Vol. 51, No. 1, pp. 124-142, 2009.

38. Sivarao, M., Amarnath, M. S., Rizal, A. K., "An Investigation Toward Development Of Economical Brake Lining Wear Alert System," International Journal of Engineering & Technology, Vol. 9, No. 9, pp. 251-256, 2009.

39. Kuciej, M. and Grzes, P., "The comparable analysis of temperature distributions assessment in disc brake obtained using analytical method and fe model," Journal of kones powertrain and transport, Vol. 18, No. 2, 2011.

40. Cho, C. and Ahn, S., "Thermo-elastic analysis for chattering phenomenon of automotive disk brake," KSME International Journal, Vol. 15, No. 5, pp. 569-579, 2001.

41. Jung, S. P., Kim, Y. G., and Park, T. W., "A Study on thermal characteristic analysis and shape optimization of a ventilated disc," Int. J. Precis. Eng. Manuf., Vol. 13, No. 1, pp. 57-63, 2012.

42. Jung, S. P., Park, T. W., Jun, K. J., Yoon, J. W., Lee, S. H., and Chung, W. S., "A Study on the Optimization Method for a Multi-body System using the Response Surface Analysis," Journal of Mechanical Science and Technology, Vol. 23, No. 4, pp. 950-953, 2009.

43. Jung, S. P., Jun, K. J., Park, T. W., and Ahn, I. C., "An Optimum Design of a Gas Circuit Breaker Using Design of Experiments," Mechanics Based Design of Structures and Machines, Vol. 36, No. 4, pp. 346-363, 2008.

44. Jung, S. P., Park, T. W., Yoon, J. W., Jun, K. J., and Chung, W. S., "Design Optimization of Spring of a Locking Nut using Design of Experiments," Int. J. Precis. Eng. Manuf., Vol. 10, No. 4, pp. 77-83, 2009.

45. Jung, S. P., Park, T. W., and Chung, W. S., "Hot Judder Analysis of the Ventilated Disc Brake System of an Automotive," Proc. KSME Autumn Conference, pp. 548-551, 2010.

46. Jung, S. P., Park, T. W., Chai, J. B., and Chung, W. S., "Thermo-mechanical finite element analysis of hot judder phenomenon of a ventilated disc brake system," Int. J. Precis. Eng. Manuf., Vol. 12, No. 5, pp. 821-828, 2011.

47. Zhang, L., Yang, Q., Weichert, D., and Tan, N., "Simulation and Analysis of Thermal Fatigue Based on Imperfection Model of Brake Discs," PAMM, Vol. 9, No. 1, pp. 533-534, 2009.

48. Cruceanu, C., Frâne pentru vehicule feroviare (Brakes for railway vehicles), Matrixrom, pp. 388, 2007.

49. Reimpel, J., "Technologie de freinage," Vogel, 1998.

50. Gotowicki, P. F., Nigrelli, V., Mariotti, G. V., Aleksendric, D., and Duboka, C., "Numerical and experimental analysis of a pegs-wing ventilated disk brake rotor, with pads and cylinders," 10th EAEC European Automotive Congress, 2005.

51. Versteeg, H. K. and Malalasekera, W., "An Introduction to Computational Fluid Mechanics: The Finite Volume Method," Prentice Hall, 2nd Ed., 2007.

52. ANSYS, Ansys User Manual v.11, ANSYS, Inc., 1996.

53. Koetniyom, S., Brooks, P. C., and Barton, D. C., "The development of a material model for cast iron that can be used for brake system analysis," Journal of Automobile Engineering, Vol. 216, No. 5, pp. 349-362, 2002.

54. Nouby, M. and Srinivasan, K., "Parametric Studies of Disc Brake Squeal using Finite Element Approach," Jurnal Mekanikal, No. 29, pp. 52-66, 2009.

55. AbuBaker, A. R. and Ouyang, H., "Wear prediction of friction material and brake squeal using the finite element method," Wear, Vol. 264, No. 11-12, pp. 1069-1076, 2008.

56. Tirovic, M. and Day, A. J., "Disc brake interface pressure distribution," Journal of Automobile Engineering, Vol. 205, pp. 137-146, 1991.

57. Ouyang, H., Cao, Q., Mottershead, J. E., and Treyde, T, "Vibration and squeal of a disc brake: modelling and experimental results," Journal of Automotive Engineering, Vol. 217, pp. 867-875, 2003.

58. Lee, Y. S., Brooks, P. C., Barton, D. C., and Crolla, D. A., "A predictive tool to evaluate disc brake squeal propensity Part 1: The model philosophy and the contact problem," International Journal of Vehicle Design, Vol. 31, No. 289-308, 2003.

APPENDIX

Total power of braking

$$P_{tot} = P_R + P_F \tag{A.1}$$

$$P_F = \sum F_F v = (F_{FV} + F_{FH})_v \tag{A.2}$$

$$P_R = \sum F_R v = [F_{RR} + F_{RP} + F_{RA}]_v \tag{A.3}$$

According to European regulation N° 13, the control provisions of braking systems refer to a vehicle braked flat neglecting the resistance due to rolling and the slope resistance (F_{RR} and $F_{RP} = 0$).

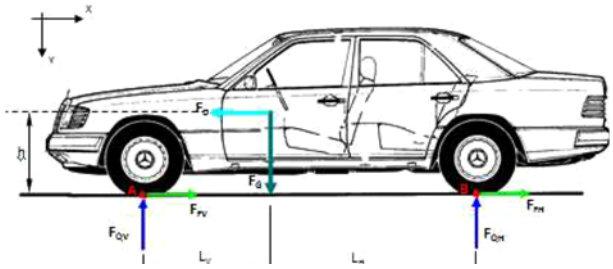

Fig. (A.1) Efforts acting on a car braking, braking of stop on flat

At speeds not exceeding 30 m/s (108 km/h) the proportion of air resistance compared to the sum of resistances does not exceed 4%. The air resistance is not important in the case of braking. For this reason ,it is negleted ($F_{RA} = 0$).

$$P_R = \sum F_R v = [F_{RR} + F_{RP} + F_{RA}]_v = 0 \tag{A.4}$$

$$P_F = \sum F_F v = (F_{FV} + F_{FH})_v \tag{A.5}$$

$$(F_{FV} + F_{FH}) = F_D = ma \tag{A.6}$$

$$P_{tot} = P_F = mav \tag{A.7}$$

Say $\varnothing$ is the coefficient that takes into account the proportion of the braking force reported to the rear wheels.

$$P_{FH} = \varnothing mav \tag{A.8}$$

$$P_F = (1-\varnothing)mav \tag{A.9}$$

For $\alpha = \text{const}$. We have:

$$v = (v_0 - at) \tag{A.10}$$

$$P_{FV} = (1-\varnothing)ma(v_0 - at) \tag{A.11}$$

Braking power reported to the brake disc.

$$P_{FV1} = \frac{(1-\varnothing)}{2} ma(v_0 - at) \tag{A.12}$$

at $t = 0$,

$$P_{FV1} = \frac{(1-\varnothing)}{2} mav_0 \tag{A.13}$$

The braking effectiveness is the relationship between deceleration (a) and acceleration (g); it is expressed generally expressed as a percentage.

$$z = A_d / g \tag{A.14}$$

$$P_{FV1} = \frac{(1-\varnothing)}{2} mgz\, v_0 \tag{A.15}$$

The heat flow to be evacuated from its surface is equal to the power friction.

In general thermal conductivity k of the material pads is smaller than that of the brake disc ($k_p < k_d$); for this reason, and also because the thermal stress calculated must be always on the side sour, it is considered that the brake disc can completely absorb the amount of produced heat.

$$Q_V = \frac{(1-\varnothing)}{2} m_{tot} gz \left[\frac{Nm}{s}\right] = [W] \tag{A.16}$$

By designating A_d the disc surface swept by a brake pad it results by holding account that the disc has two faces and on each pad is in contact, the friction power transformed by unit area is:

$$Q_V' = \frac{(1-\varnothing)}{2} \frac{m_{tot} gv}{2 A_d} \left[\frac{Nm}{sm^2}\right] = [W/m^2] \tag{A.17}$$

Size Q_V' represent the heat flux evacuated by the disc surface. It is even small; more really swept surface A_d is large. In the most favorable case it can be equal to the total area of friction ring disc. Actually, the brake pads are not in perfect contact with the brake disc.

The relation (A.17) is not longer valid, we introduce a factor called factor of exploitation ε_p of rubbing surface:

$$\varepsilon_p = \frac{Q_V'}{Q_{V'max}} \tag{A.18}$$

The maximum heat flux crossing the surface friction useful is calculated as follows:

$$Q_{V'max} = \frac{(1-\varnothing)}{2} \frac{m_{tot}}{2} \frac{gv}{A_d \varepsilon_p} \left[\frac{Nm}{sm^2}\right] = [W/m^2] \tag{A.19}$$

ε_p :Factor taking account of the load distribution on the disc surface.

- In the case of the Dunlop caliper type ε_p can grow up to 0.9,
- For fixed caliper with double pistons ε_p are equal to about 0.7,
- For the plunger caliper ε_p rarely exceed 0.5.

The heat flux determined by the equation (A.19) is the initial heat flux entering. It varies very quickly even with a constant deceleration ($z = const$), because during braking, speed v decreases. It is therefore about a steady state problem, which cannot be solved only by the numerical methods.